

# Heavy Flavor in Photoproduction at HERA

---

Leonid Gladilin<sup>\*†</sup>

DESY, Notkestr. 85, 22603 Hamburg, Germany

E-mail: gladilin@mail.desy.de

ABSTRACT: Recent results on charm and beauty photoproduction at HERA are discussed. The perturbative QCD calculations are generally smaller than the measured cross sections, particularly in the forward (proton) direction. The study of charm dijet photoproduction is consistent with a significant contribution of charm excitation processes.

---

## 1. Introduction

During the first phase of operation (1992–2000), HERA collided electrons and positrons with energy 26.7 – 27.6 GeV and protons with energy 820 – 920 GeV yielding a center-of-mass energy of 296 – 318 GeV. In this period, extensive measurements of heavy flavor photoproduction were made by the H1 and ZEUS collaborations [1, 2, 3, 4, 5]. Some recent charm and beauty photoproduction results are discussed in this paper.

In photoproduction processes at HERA, a quasi-real photon with virtuality  $Q^2 \sim 0$  is emitted by the incoming electron and interacts with the proton. At leading order (LO) in QCD, two types of processes are responsible for the production of heavy quarks: the direct photon processes, where the photon participates as a point-like particle, and the resolved photon processes, where the photon acts as a source of partons. The dominant direct photon process is photon-gluon fusion where the photon fuses with a gluon from the incoming proton. In resolved photon processes, a parton from the photon scatters off a parton from the proton. Charm and beauty quarks present in the parton distributions of the photon, as well as of the proton, lead to processes like  $cg \rightarrow cg$  and  $bg \rightarrow bg$ , which are called heavy flavor excitation processes. In next-to-leading order (NLO) QCD, only the sum of direct and resolved processes is unambiguously defined.

## 2. Charm photoproduction

Differential cross sections for  $D^{*\pm}$  and  $D_s^\pm$  photoproduction in  $p_\perp^D$  and  $\eta^D$  were measured in the kinematic range  $Q^2 < 1 \text{ GeV}^2$ ,  $130 < W < 280 \text{ GeV}$ ,  $3 < p_\perp^D < 12 \text{ GeV}$  and

<sup>\*</sup>Speaker.

<sup>†</sup>On behalf of the H1 and ZEUS Collaborations.

$|\eta^D| < 1.5$  [2, 3]. Here  $W$  is the  $\gamma p$  center-of-mass energy, and  $p_\perp^D$  and  $\eta^D$  are the  $D$ -meson transverse momentum and pseudorapidity, respectively. The pseudorapidity  $\eta$  is defined as  $-\ln(\tan \frac{\theta}{2})$ , where the polar angle  $\theta$  is measured with respect to the proton beam direction.

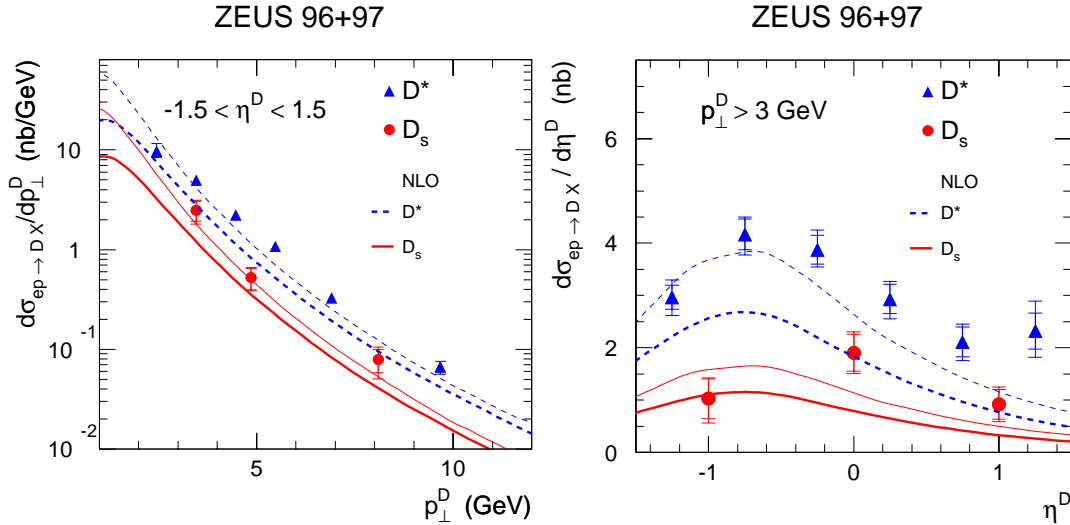


**Figure 1:** Differential cross sections  $d\sigma/p_\perp^D$  (left) and  $d\sigma/d\eta^D$  (right) for  $D_s^\pm$  and  $D^{*\pm}$  photoproduction. The  $D_s^\pm$  (dots) and  $D^{*\pm}$  (triangles) data are compared with NLO predictions for  $D_s^\pm$  (full curves) and  $D^{*\pm}$  (dashed curves).

In Fig. 1, NLO calculations [6] obtained with the MRS(G) and GRV-G HO [7] parton density parametrisations for the proton and photon, respectively, are compared with the differential cross sections. The thick curves were obtained with the renormalization scale  $\mu_R = m_\perp \equiv \sqrt{m_c^2 + p_\perp^2}$  ( $m_c = 1.5$  GeV) and the factorization scales of the photon and proton structure functions were set to  $\mu_F = 2m_\perp$ . For the thin curves, a rather extreme value for the pole  $c$ -quark mass,  $m_c = 1.2$  GeV, and a  $\mu_R$  value of  $0.5m_\perp$  were used. The Peterson fragmentation function [8] was used for charm fragmentation in this calculation. Following the results of the NLO fits [9] to ARGUS data [10], the same values of the Peterson parameter,  $\epsilon = 0.035$ , were used for both  $D^{*\pm}$  and  $D_s^\pm$  cross section calculations. The fractions of  $c$  quarks hadronizing as  $D^{*\pm}$  or  $D_s^\pm$  mesons were extracted from results on charm production in  $e^+e^-$  annihilations [11]. The NLO calculations underestimate the measured cross sections. The shapes of the  $p_\perp^D$  distributions are not completely reproduced. For the  $\eta^D$  distributions, the NLO predictions are below the data in the central and forward (proton direction) regions.

An experimental separation of the direct and resolved processes was obtained by using the variable  $x_\gamma^{\text{obs}}$ , which is the fraction of the photon momentum contributing to the production of the two jets with the highest transverse energies within the accepted pseudorapidity range. The charm photoproduction differential cross section was measured as a function of  $x_\gamma^{\text{obs}}$  [2]. A comparison of the  $x_\gamma^{\text{obs}}$  distribution with LO Monte Carlo (MC) simulations indicated the existence of charm excitation in the photon parton density. Recently, the ZEUS collaboration has performed new measurements of charm dijet photoproduction [12]. The angle between the jet-jet axis and the beam axis in the dijet rest frame has

been approximated by the variable  $\cos\theta^*$ , which is a function of the pseudorapidities of the two jets:

$$\cos\theta^* = \tanh\left(\frac{\eta^{jet1} - \eta^{jet2}}{2}\right).$$

In the previous inclusive dijet analysis [13], it was shown that in direct photon processes, where the propagator in the leading-order (LO) QCD diagrams is a quark, the differential cross section  $d\sigma/d|\cos\theta^*|$  rises slowly towards values of  $|\cos\theta^*| \sim 1$ , while in resolved photon processes, where in most cases the propagator is a gluon, it rises steeply with increasing  $|\cos\theta^*|$ , consistent with the behavior of a spin-1 propagator.

The differential distribution  $dN/d|\cos\theta^*|$  for events with at least two jets and a  $D^{*\pm}$  is shown in Fig. 2. The data points are given separately for direct photon (open dots) and for resolved photon (black dots) events. In this analysis, a direct (resolved) photon process was defined by the selection  $x_\gamma^{\text{obs}} > 0.75$  ( $x_\gamma^{\text{obs}} < 0.75$ ). The dashed (full) histogram is the PYTHIA [14] distribution for the direct (resolved) photon MC events. All the distributions are normalized to the resolved data distribution in the first 4 bins. An enhancement at high values of  $|\cos\theta^*|$  is seen for the resolved photon sample, both in the data and in the MC simulation. The direct photon samples do not show this strong peaking. This observation is consistent with a significant gluon-exchange contribution and, consequently, with a significant contribution of charm excitation processes to charm photoproduction at HERA energies.

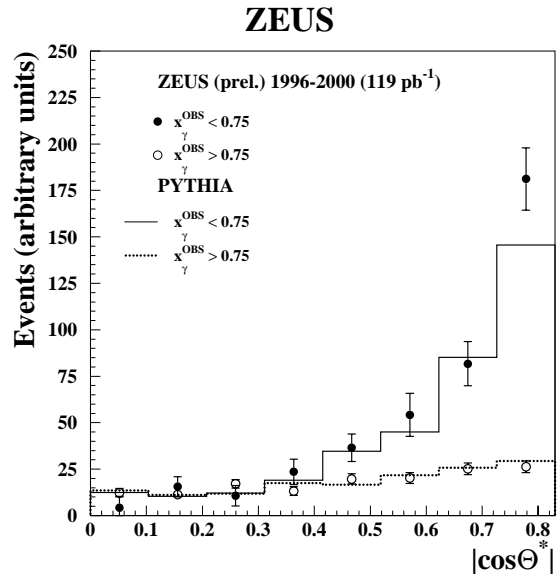


**Figure 2:** Differential distributions  $dN/d|\cos\theta^*|$  for the data (dots) and PYTHIA MC simulation (lines).

### 3. Beauty photoproduction

Beauty photoproduction cross sections were measured by the H1 and ZEUS collaborations using events with at least two jets and a lepton in the final state [4, 5]. The beauty signals were extracted by fitting the  $p_T^{\text{rel}}$  distributions of the data with Monte Carlo predictions for beauty and the lighter flavor components, where  $p_T^{\text{rel}}$  is the transverse momentum of the lepton relative to the axis of the associated jet. The cross sections were found to be above NLO QCD expectations.

Recently, the H1 collaboration has performed new measurements of the beauty photoproduction using a central silicon vertex detector [15]. The cross section was extracted from the  $p_T^{\text{rel}}$  and impact parameter ( $\delta$ ) distributions of muons in dijet events. Fig. 3 shows the observed impact parameter distribution in the data together with histograms indicating the contributions from beauty production and from backgrounds. The decomposition

was obtained from a likelihood fit using the shapes of the  $\delta$  distributions of beauty and charm events from Monte Carlo simulations and of fake muons from real data. Using both  $p_T^{\text{rel}}$  and  $\delta$  observables, and in combination with the earlier result, the open beauty cross section was determined in the visible range  $Q^2 < 1 \text{ GeV}^2$ ,  $0.1 < y < 0.8$ ,  $p_{\perp}^{\mu} > 2.0 \text{ GeV}$ ,  $35^{\circ} < \theta^{\mu} < 130^{\circ}$ :  $\sigma_{\text{vis}}(ep \rightarrow b\bar{b}X \rightarrow \mu X) = (170 \pm 25) \text{ pb}$ .

The NLO QCD prediction, using the fixed-order NLO calculation [6] and a fragmentation parameterization described in [4], is  $(54 \pm 9) \text{ pb}$ , where the error was estimated by varying the renormalization and factorization scales, the beauty quark mass value and the fragmentation parameters. The NLO prediction undershoots the measured cross section significantly.

The ZEUS collaboration has recently performed the first measurement of the beauty photoproduction differential cross sections [16]. Events with a muon and at least two jets were selected. Differential cross sections as a function of the muon pseudorapidity,  $\eta^{\mu}$ , and transverse momentum,  $p_T^{\mu}$ , were calculated. The beauty fraction in each bin of the selected variable was extracted with the  $p_T^{\text{rel}}$  fit.

Fig. 4 shows the measured beauty differential cross sections in comparison with predictions of PYTHIA [14] and HERWIG [17]. The PYTHIA predictions are in reasonable agreement with the data. The agreement is worse in the most-forward  $\eta^{\mu}$  bin, in which the contribution from the beauty excitation processes is expected to be large. As shown, the beauty excitation is a substantial component of the PYTHIA cross section. The HERWIG predictions, which also include the beauty excitation component, are lower than PYTHIA but still compatible with the data within errors.

#### 4. Summary

Charm and beauty photoproduction cross sections have been measured by the H1 and ZEUS collaborations. The perturbative QCD calculations are generally smaller than the measured cross sections, in particular in the forward (proton) direction. In the charm sector, theoretical uncertainties are larger than the experimental ones. The study of dijet photoproduction associated with charm is consistent with a significant contribution of charm excitation processes.

#### References

- [1] C. Adloff et al. [H1 Collaboration], *Nucl. Phys.* **B 545** (1999) 21.

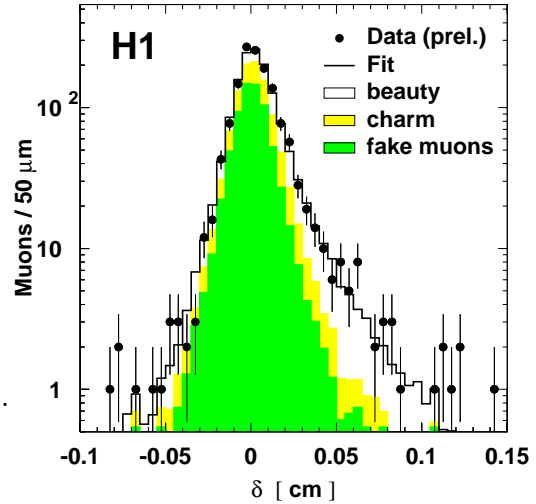


**Figure 3:** Muon impact parameter distribution and decomposition from the likelihood fit.

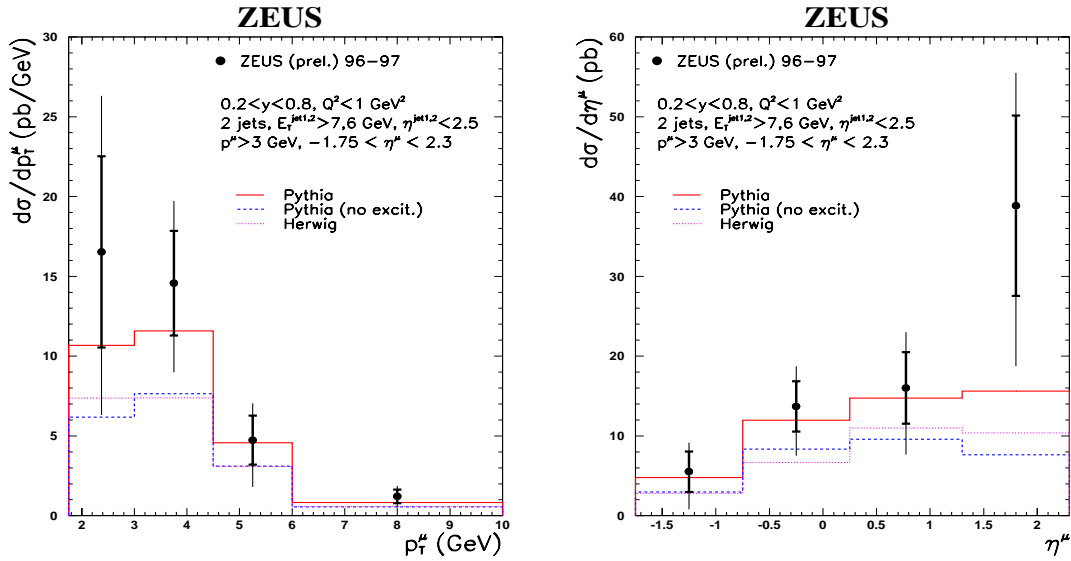


**Figure 4:** Differential beauty cross sections  $d\sigma/p_T^\mu$  (left) and  $d\sigma/d\eta^\mu$  (right) for events with two jets and a muon, compared to predictions of PYTHIA and HERWIG MC programs.

- [2] J. Breitweg et al. [ZEUS Collaboration], *Eur. Phys. J. C* **6** (1999) 67.
- [3] J. Breitweg et al. [ZEUS Collaboration], *Phys. Lett. B* **481** (2000) 213.
- [4] C. Adloff et al. [H1 Collaboration], *Phys. Lett. B* **467** (1999) 156; erratum. *ibid.* **518** (2001) 331.
- [5] J. Breitweg et al. [ZEUS Collaboration], *Eur. Phys. J. C* **18** (2001) 625.
- [6] S. Frixione et al., *Nucl. Phys. B* **454** (1995) 3.
- [7] H. Plochow-Besch, *Int. J. Mod. Phys. A* **10** (1995) 2901.
- [8] C. Peterson et al., *Phys. Rev. D* **27** (1983) 105.
- [9] P. Nason and C. Oleari, *Phys. Lett. B* **447** (1999) 327 and hep-ph/9903541.
- [10] H. Albrecht et al. [ARGUS Collaboration], *Z. Physik C* **52** (1991) 353; *ibid.* **54** (1992) 1.
- [11] L. Gladilin, hep-ex/9912064, 1999.
- [12] S. Chekanov et al. [ZEUS Collaboration], contrib. paper no. 499 to this conference.
- [13] M. Derrick et al. [ZEUS Collaboration], *Phys. Lett. B* **384** (1995) 401.
- [14] T. Sjöstrand, *Comput. Phys. Commun.* **82** (1994) 74.
- [15] C. Adloff et al. [H1 Collaboration], contrib. paper no. 311 to ICHEP 2000, Osaka, Japan.
- [16] S. Chekanov et al. [ZEUS Collaboration], contrib. paper no. 496 to this conference.
- [17] G. Marchesini et al., *Comput. Phys. Commun.* **67** (1992) 465.